Involvement of Hippocampal Inputs and Intrinsic Circuit in the Acquisition of Context and Cues During Classical Conditioning in Behaving Rabbits

Alejandro Carretero-Guillén, Renny Pacheco-Calderón, José M. Delgado-García and Agnès Gruart

Division of Neurosciences, Pablo de Olavide University, E-41013 Seville, Spain

Address correspondence to Prof. Agnès Gruart, Division of Neurosciences, Pablo de Olavide University, Carretera de Utrera, Km. 1, Seville-41013, Spain. Email: agrumas@upo.es

Learning-related changes in strength in selected hippocampal synapses have been described recently. However, information is scarce regarding the spatial-temporal sequence of changes in synaptic weights taking place during the acquisition of a classical conditioning task and the contribution of both context (environmental details) and cues (conditioned and unconditioned stimuli: CS, US) to those activity-dependent changes. We recorded in rabbits the monosynaptic field excitatory postsynaptic potentials (fEPSPs) evoked at 6 different hippocampal synapses during the acquisition and extinction of a classical eyeblink conditioning using trace or delay paradigms, as well as during pseudoconditioning and in the absence of CS and US presentations (context). Context and pseudoconditioning training evoked early, lasting changes in synaptic strength in perforant pathway synapses in dentate gyrus (PP-DG), and hippocampal CA3 (PP-CA3) and CA1 (PP-CA1) areas. Pseudoconditioning also evoked early, nonlasting changes in strength within the intrinsic hippocampal circuit (CA3-CA1 and CA3-cCA1 synapses). In contrast, during both trace and delay training sessions, synaptic changes in strength were mostly noticed within the intrinsic hippocampal circuit (DG-CA3, CA3-CA1, CA3-cCA1). The response of hippocampal synapses to afferent impulses seems to be modulated by both context and cues during associative learning in behaving rabbits.

Keywords: associative learning, behaving rabbits, changes in synaptic strength, hippocamapal synapses, neuronal plasticity

Introduction

One of the more basic tenets of current neuroscience is that newly acquired motor and/or cognitive abilities are stored in the form of functional and structural changes in synaptic efficiency (Ramón y Cajal 1909–1911; Konorski 1948; Hebb 1949). In this regard, convincing relationships have been shown between acquired learning abilities in experimental animals and the underlying changes in synaptic activity, determined by genetic, molecular, and *in vitro* electrophysiological studies (Bliss and Collingridge 1993; Kandel 2001; Neves et al. 2008; Wang and Morris 2010). Nevertheless, functional changes evoked by learning should be susceptible to being detected at synapses relevant to the learning process. For example, activity-dependent changes in synaptic strength have been reported in behaving mammals during the very moment of the acquisition process (Gruart et al. 2006; Whitlock et al. 2006). However, 2 important questions remain to be addressed: Are all synapses of large cortical circuits behaving in the same way during the acquisition and extinction processes? And, are activity-dependent changes in synaptic strength involved only in the relevant association cues or is the context also relevant in the learning process?

Of the cerebral cortical structures, the hippocampus has been one of the most studied, being implicated in a wide variety of learning and memory experimental paradigms, including object recognition (Clarke et al. 2010), spatial orientation (Moser et al. 2008; Wang and Morris 2010), and classical conditioning of eyelid responses (Berger et al. 1983; McEchron and Disterhoft 1997; Múnera et al. 2001). Indeed, firing activities of identified hippocampal CA3 and CA1 pyramidal neurons recorded in behaving cats are related to the acquisition of classical conditioning of eyelid responses, using both trace and delay paradigms (Múnera et al. 2001). But, here again, there is no complete information on the global activity of hippocampal circuits during the same type of associative learning.

In order to address these issues, we decided to determine in behaving rabbits the changes in synaptic strength of selected hippocampal synapses taking place during different classical conditioning protocols. Following the earlier demonstration with regard to perforant pathway projections in dentate gyrus (PP-DG; Weisz et al. 1984) and CA3-CA1 (Gruart et al. 2006) synapses, we studied here whether the acquisition of a classical conditioning task modifies the synaptic weights in 4 additional hippocampal synapses: PP-CA3, PP-CA1, DG-CA3, and CA3-cCA1). For this, we trained rabbits for a classical conditioning of eyelid responses, with both trace and delay paradigms, presenting a tone as CS and an air puff aimed at the cornea as US. Animals were also trained for pseudoconditioning and just to the context situation (i.e., in the absence of CS and/or US presentations). Conditioned responses (CRs) were determined from the electromyographic (EMG) activity of the orbicularis oculi muscle. We recorded field excitatory postsynaptic potentials (fEPSPs) evoked at the 6 hippocampal synapses during the 4 experimental situations. For this, animals were chronically implanted with multiple recording and stimulating electrodes in the selected intra- and extrahippocampal sites. Present results provide substantial evidence of the intrinsic relationships between activity-dependent synaptic changes in strength in the hippocampal circuits and context and cues present in associative learning tasks in mammals.

Materials and Methods

Experimental Animals

Experiments were carried out on adult male rabbits (New Zealand white albino) weighing 2.6–3.1 kg on arrival, obtained from an authorized supplier (Isoquimen, S.L., Barcelona, Spain). Animals were housed in individual cages for the whole experiment, and kept on a 12/12 h light/dark cycle with constant ambient temperature (21 ± 1 °C) and humidity (50 ± 7%). Food and water were available *ad libitum*. All experimental procedures were carried out in accordance with the guidelines of the European Union Council (2003/65/CE) and Spanish (BOE 252/34367-91, 2005) regulations for the use of laboratory animals in chronic experiments. Experimental protocols were also approved by the local University Ethics Committee.

Surgery

Animals were anesthetized with a ketamine-xylazine cocktail (ketaminol, 50 mg/mL; rompun, 20 mg/mL; and atropine sulfate, 0.5 mg/kg). Animals were prepared for the chronic recording of fEPSPs evoked at selected sites within the dorsal hippocampus (Fig. 1A). For this, animals were implanted with bipolar stimulating electrodes in the perforant pathway, the dentate gyrus, or the hippocampal CA3 area, and with recording electrodes aimed at the dentate gyrus, and/or the hippocampal CA3 and CA1 areas (see location and coordinates in Fig. 1B, C,E; Girgis and Shih-Chang 1981). Each animal was implanted with
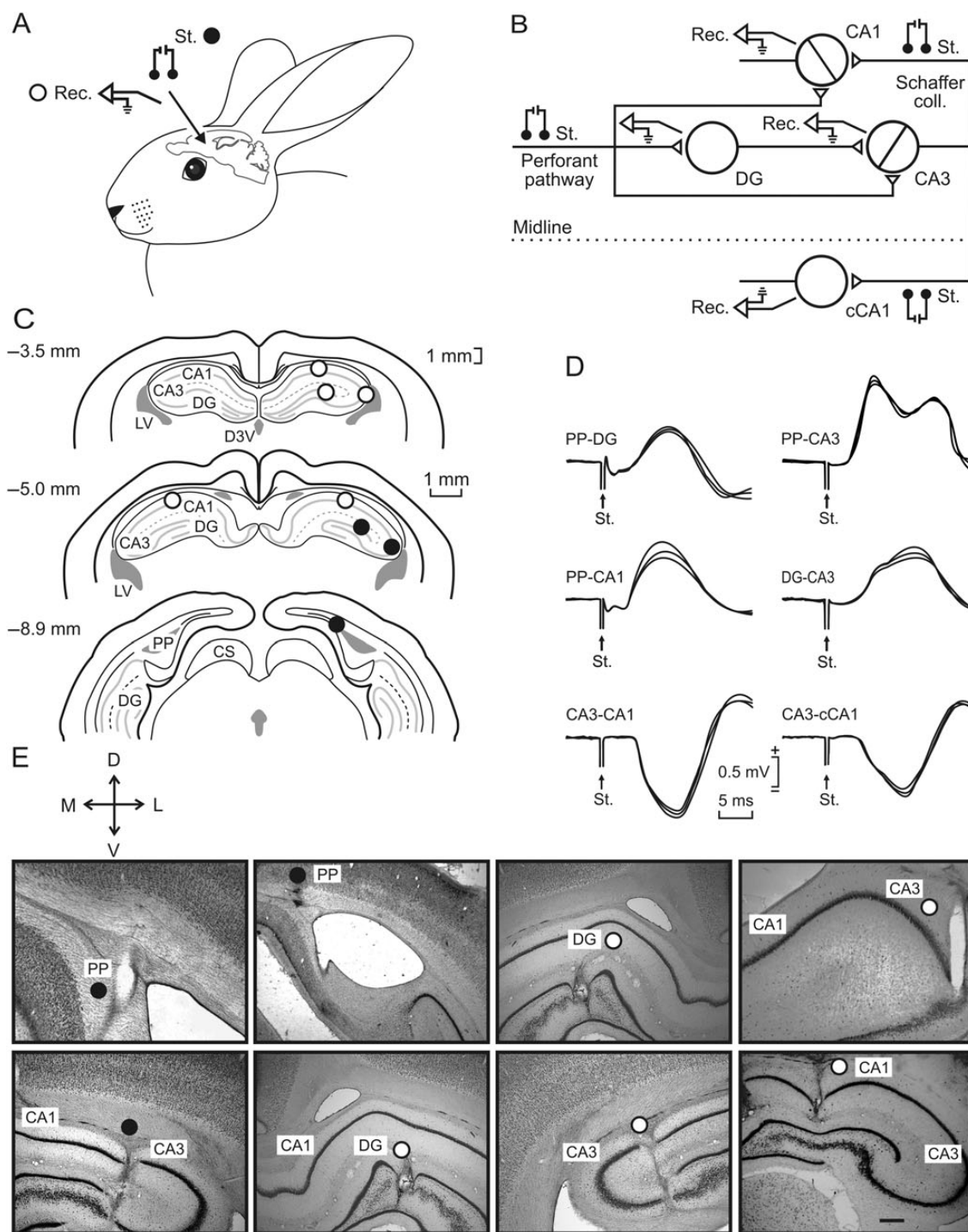

Figure 1. Experimental design. (*A,B*) For the classical conditioning of eyelid responses, rabbits were chronically implanted with recording (Rec.) electrodes in the right dentate gyrus (DG) and hippocampal CA1 and CA3 areas, as well as in the contralateral CA1 (cCA1) area. Animals were also implanted with stimulating (St.) electrodes in the perforant pathway and in the ipsi- and contralateral Schaffer collateral/commissural pathway. (*C*) Schematic diagrams in stereotaxic coordinates from rabbit brain (modified from Girgis and Shih-Chang 1981) with indication of selected recording (white circles) and stimulating (black circles) sites. (*D*) Representative records collected from the 6 (PP-DG, PP-CA3, PP-CA1, DG-CA3, CA3-CA1, and CA3-cCA1) synapses included in this study. Calibration at the bottom is for all records. (*E*) Different photomicrographs illustrating the final location of stimulating (black circles) and recording (white circles) electrodes. Calibration bar is 1 mm. D, L, M, V, dorsal, lateral, medial, ventral; CS, superior colliculus; D3 V, dorsal part of the third ventricle; LV, lateral ventricle; PP, perforant pathway.

several (up to 3) stimulating and (up to 16) recording electrodes. Stimulating (bipolar) and recording (tetrode) electrodes were made from 50 μm, Teflon-coated tungsten wire (Advent Research Materials Ltd., Eynsham, England). Tetrode diameter was ≈ 110 μm. The impedance of recording electrodes was always >1 MΩ. The final position of hippocampal stimulating and recording electrodes was determined under recording procedures until a reliable monosynaptic field EPSP was identified (Fig. 1D; see Gruart et al. 2006 for details). All the animals were also implanted with recording bipolar hook electrodes in the left orbicularis oculi muscle to record its EMG activity (Fig. 2A). These electrodes were made from Teflon-coated stainless steel wire (A-M Systems, Sequim, WA, USA) with an external diameter of 50 μm. A silver electrode (1 mm in diameter) was attached to the skull (occipital bone) as a ground. Terminals of hippocampal stimulating and recording, EMG, and ground electrodes were soldered to three 9-pin sockets. All wire connections were covered with cyanoacrylate glue, and the whole system was attached to the skull with the aid of 3 small screws fastened and cemented with an acrylic resin to the bone (for details see Leal-Campanario et al. 2007).

Recording and Stimulation Procedures

Recording sessions began 2 weeks after surgery. The animal was placed in a Perspex box specially designed for limiting the subject's movements (Gruart et al. 2000). The box was placed on the recording table and covered by a black cloth. The recording room was kept softly illuminated, and a 60-dB background white noise was switched on during the experiments. Animals were divided in 4 experimental groups: context, pseudoconditioning, and trace and delay conditioning.

The EMG activity of the selected muscle was recorded using Grass P511 differential amplifiers with a bandwidth of 0.1 Hz to 10 kHz (Grass-Telefactor, West Warwick, RI, USA). FEPSPs were recorded with a 16-channel extracellular differential AC amplifier (Model 3500, A-M Systems) provided with a head-stage interface adapter.

Air puffs aimed at the left cornea were applied through the opening of a plastic pipette (3 mm in diameter) attached to a metal holder fixed to the animal's 9-pin socket (Dual-channel air-puff device, Biomedical Engineering, Co.). Tones were applied from a loudspeaker located 80 cm below the animal's head. Electrical stimulation of the selected sites was achieved with a CS-220 stimulator across an ISU-220 isolation unit
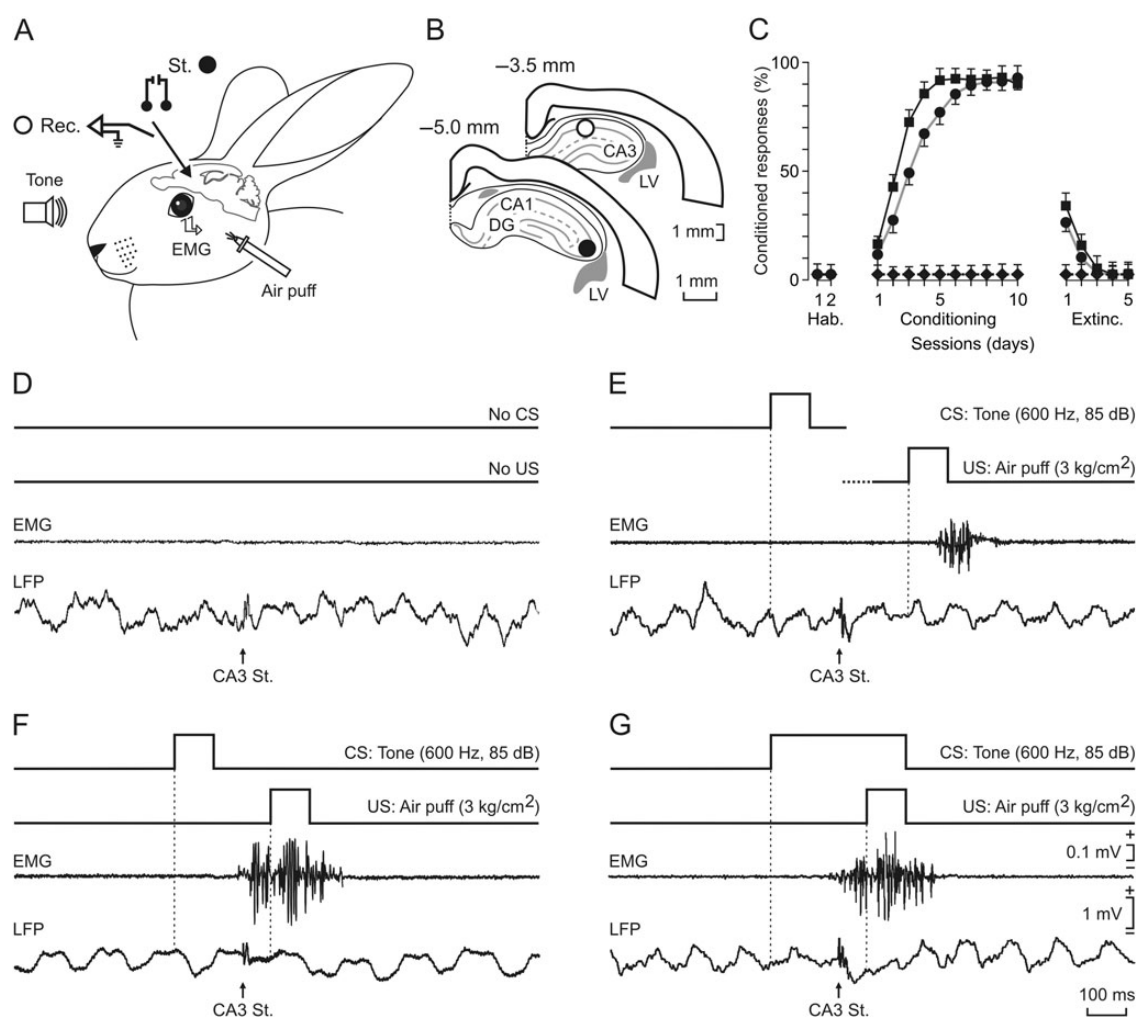
Figure 2. Classical conditioning paradigms. (A) In addition to hippocampal stimulating and recording electrodes (Fig. 1), animals were implanted with EMG recording electrodes in the left orbicularis oculi muscle. For classical eyeblink conditioning, the US consisted of an air puff presented to the ipsilateral cornea, while the CS consisted of tones presented biaurally. (B–G) Animals were presented with 4 different training situations: 1) placed in the restraining box with no CS or US presentations (D); 2) pseudoconditioning (E) with non-paired CS and US presentations; 3) a trace conditioning paradigm (F); and, 4) a delay conditioning paradigm (G). In D–G and from top to bottom are illustrated CS and US presentations, the EMG activity of the orbicularis oculi muscle, and the local field potential recorded in the CA1 area (white circle in B), as well as the fEPSP evoked by a stimulus presented to the ipsilateral Schaffer collaterals (black circle in B). Calibrations in G are also for (D–F). Note that only trace and delay conditioning evoked CRs. The corresponding learning curves evoked by pseudoconditioning (black diamonds), and trace (black circles) and delay (black squares) paradigms are illustrated in (C), during the successive habituation (Hab.), conditioning, and extinction (Extinc.) sessions.

(Cibertec, Madrid, Spain). Single (cathodal, square, 50 μs, <1 mA pulses) or paired (40 of interpulse interval) stimuli were programmed.

Classical Eyeblink Conditioning

Conditioning consisted of 2 habituation, 10 conditioning, and 5 extinction sessions. The trace conditioning paradigm consisted of a 100 ms, 600 Hz, 85 dB tone followed 250 ms after CS onset by a 100 ms, 3 kg/cm^2 air puff aimed at the left cornea; thus, a trace interval of 150 ms was left between CS end and US onset. In the delay paradigm, the CS consisted of a 350 ms, 600 Hz, 85 dB tone. The US started 250 ms after CS onset, and consisted of a 100 ms, 3 kg/cm^2 air puff aimed at the left cornea; in this case, the US co-terminated with the CS. Conditioning sessions consisted of 66 trials (6 series of 11 trials each) separated at random by intervals of 50–70 s. Of the 66 test trials, 6 were trials in which the CS was presented alone. A complete conditioning session lasted for ~ 1 h. The CS was presented alone during habituation and extinction sessions for the same number of blocks/session and trials/block. As criterion, we considered a "CR" the presence—during the CS-US interval—of EMG activity lasting >10 ms and initiated >50 ms after CS onset. In addition, the integrated EMG activity recorded during the CS–US interval had to be at least 1.2 times greater than the integrated EMG recorded immediately before CS presentation (Porras-García et al. 2010). As a criterion for learning, animals should evoke >70% CRs by the 10th conditioning session (Gruart et al. 2000; Leal-Campanario et al. 2007).

For context sessions, the animal was set in the restraining box for 1 h during a total of 17 sessions. No CS or US were presented during context sessions. For pseudoconditioning, unpaired CS and US were presented for 10 sessions (66 times/session) preceded by 2 and followed by 5 sessions during which the CS was presented alone. Pseudoconditioned animals also received 2 habituation and 5 extinction sessions as indicated above.

For trace and delay conditioning, as well as for pseudoconditioning, animals were stimulated in the selected brain sites at 200-ms following CS presentation. In the context group, animals were stimulated at random by intervals of 50–70 s for a total of 66 times.

Histology

At the end of the experiments, animals were deeply anesthetized with sodium pentobarbital (50 mg/kg, i.p.), and perfused transcardially with saline and 4% paraformaldehyde. In order to determine the final location of recording and stimulation sites, the brain was removed and cut into slices (50 μm), and the relevant brain areas were processed for Nissl (toluidine blue) staining (Fig. 1E).

Data Collection and Analysis

fEPSPs, the unrectified EMG activity of the recorded muscles, and 1-V rectangular pulses corresponding to CS, US, and electrical stimuli presented during the different experimental situations, were acquired on-line through an 8-channel analog-to-digital converter (CED 1401-plus, CED, Cambridge, UK), and transferred to a computer for quantitative offline analysis. Data were sampled at 8000 Hz (for fEPSP recordings) or 4000 Hz (for EMG recordings), with an amplitude resolution of 12 bits. Computer programs (Spike2 and SIGAVG from CED) were used to analyze field potentials and EMG activities. These programs allowed the quantification, with the aid of cursors, of the onset latency and area (mV × s) of the rectified EMG activity of the orbicularis oculi muscle. Field synaptic potentials (in mV) collected from the same session ($n = 66$) and animal were averaged, and the mean value of the slope (in mV/s) was determined for the rise time period (i.e., the period of the slope between the initial 10% and the final 10% of the evoked field potential).

Statistical analyses were performed using the Sigma Plot 11.0 package (Sigma Plot, San Jose, CA, USA), for a statistical significance level of $P = 0.05$. Unless otherwise indicated, mean values were calculated from ≥15 electrodes, collected from 6 animals. Mean values are followed by their standard error. Nonlinear regression analysis was used to study the evolution of fEPSP slopes across conditioning sessions (Fig. 3E) for the 4 experimental conditions. Collected data were analyzed using the one-way or two-way ANOVA test, with time or session as repeated measure, coupled with contrast and/or nonparametric analysis when appropriate. Repeated-measures ANOVA allowed checking the statistical differences of the same group across sessions. The Student t-test was used when necessary.

Results

Experimental Design and Identification of Stimulation and Recording Sites

As illustrated in Figure 1A, animals were prepared for the chronic recording of fEPSPs evoked in the neuronal components of the hippocampal intrinsic circuit by the electrical stimulation of the main afferent input to the hippocampus (i.e., the perforant pathway) or of some defined axonal projections inside the intrinsic circuit. In accordance with data collected from some preliminary experiments, we selected the following 6 synapses (Fig. 1B): the PP-DG and the hippocampal CA3 (PP-CA3) and CA1 (PP-CA1) areas, the dentate gyrus projection to the CA3 area (DG-CA3), the Schaffer collateral projection to CA1 pyramidal cells (CA3-CA1), and CA3 projections to contralateral CA1 neurons (CA3-cCA1). Stimulating and recording electrodes were implanted in the dorsal hippocampus at the sites illustrated in Figure 1C. Selected stereotaxic coordinates were collected from the atlas of Girgis and Shih-Chang (1981) and adjusted to obtain well-defined fEPSPs with minimum intensities (<1 mA). Figure 1D illustrates a set of representative fEPSPs evoked at the 6 selected synapses. In most of the cases, recorded fEPSPs presented latencies <6 ms —i.e., well in the range of or slightly shorter than those in classical reports of recordings of the same monosynaptic fEPSPs carried out in anesthetized rabbits (Andersen et al. 1966a,b; Lømo 1971a,b). Recorded fEPSPs presented positive or negative components depending on the location of the recording electrode with respect to the soma or dendrites of the postsynaptic element (Andersen et al. 1966a,b; Lømo 1971a,b; Bliss and Lømo 1973). Characteristically, fEPSPs evoked at the PP-CA3 synapse presented a second positive (or negative) component, indicating the secondary activation of pyramidal CA3 cells by DG afferents to them (Fig. 1D, top-right recordings). Finally, Figure 1E illustrates the proper location of stimulating and recording electrodes.

Context, Pseudoconditioning, and Trace and Delay Conditioning Paradigm Groups

For animal training, animals were additionally implanted with bipolar EMG recording electrodes in the left orbicularis oculi muscle—i.e., in the side contralateral to the hippocampal electrodes (Fig. 2A,B). Rabbits ($n = 6$ per group) were presented with the following paradigms: 1) Context situation: Animals were placed in the restraining box for 1 h/day for a total of 17 sessions; no CS or US were presented to them (Fig. 2D). 2) Pseudoconditioning: Animals were placed in the restraining box for 2 habituation, 10 pseudoconditioning, and 5 extinction sessions (Fig. 2E). iii) Trace paradigm: Animals were trained with the trace paradigm described in Materials and Methods (Fig. 2F). And, iv) Delay paradigm: These animals were trained with the delay paradigm described in Materials and Methods (Fig. 2G).

In all cases, sessions lasted for 1 h and a total of 66 paired (or unpaired) CS and US stimuli were presented during the
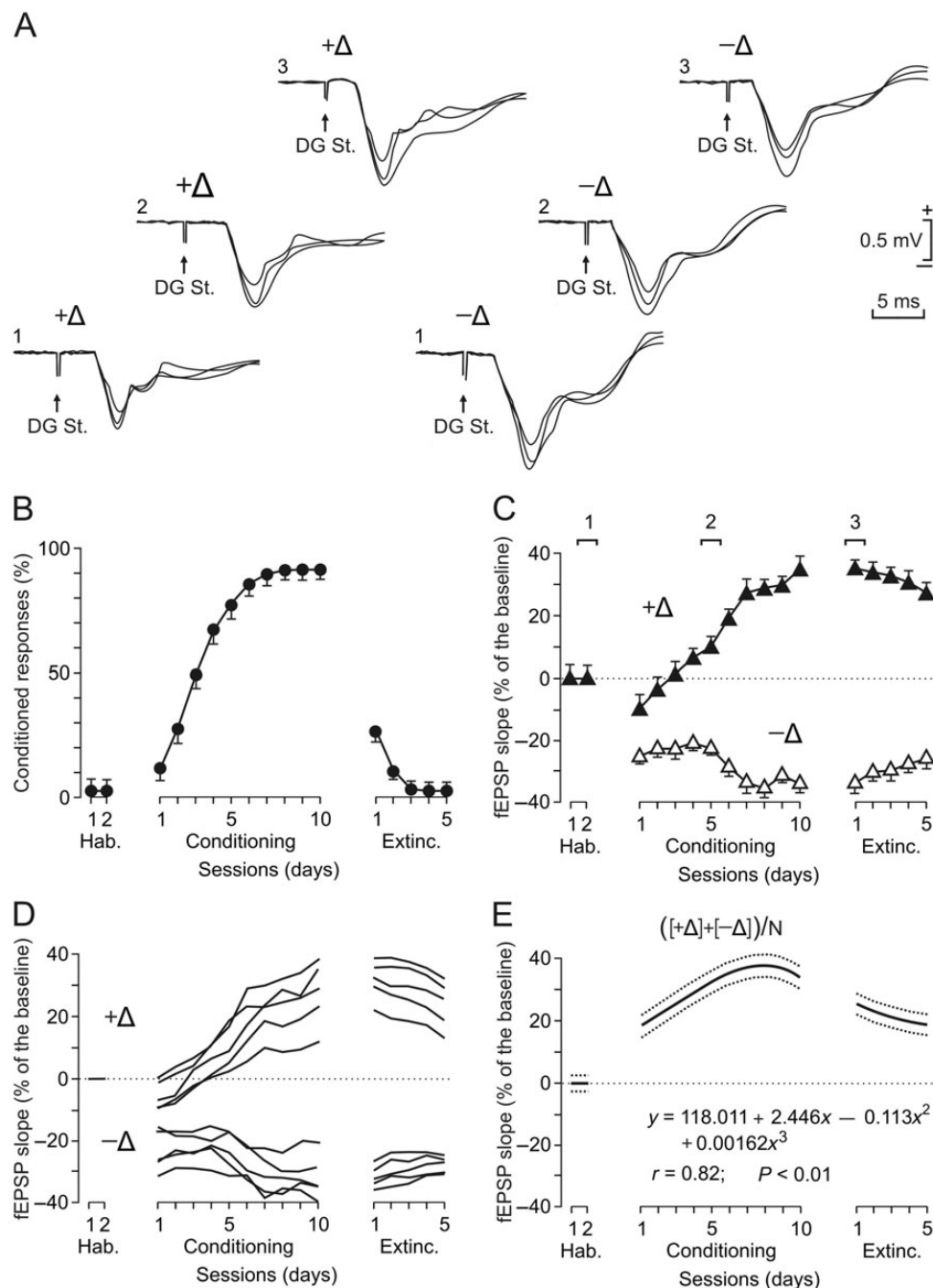
Figure 3. Results collected at the hippocampal DG-CA3 synapse during classical eyeblink conditioning using a trace paradigm. (*A*) Representative examples of fEPSPs recorded from 2 different electrodes located in the hippocampal CA3 area and evoked by the electrical stimulation of the ipsilateral DG. (*B*) Evolution of CRs in the group of rabbits (*n* = 6) trained with a trace paradigm. (*C*) Evolution of fEPSP slopes, recorded from two different electrodes implanted in the CA3 area, across the successive training sessions illustrated in (*B*). Representative examples of the recorded fEPSPs at the indicated times (1, 2, 3) are illustrated in A for the 2 recording sites. (*D*) Evolution of fEPSP slopes recorded from selected electrodes implanted in the CA3 area. fEPSPs were evoked by the electrical stimulation of the ipsilateral DG. Note that fEPSPs either increase (+Δ, *n* = 5) or decrease (−Δ, *n* = 5) in slope across training. (*E*) Algebraic mean [([+Δ] + [−Δ])/*N*] of fEPSP evolution from electrodes (*n* = 15) located in the hippocampal CA3 area and activated by DG stimulation. The equation corresponding to the best polynomial fit to data collected during conditioning sessions is indicated, as well as the corresponding regression curve and the simultaneous 95% confidence bands.

session. As illustrated in Figure 2B,D–G, animals of the 4 groups were stimulated at a minimum of 1, or a maximum of 3, hippocampal synapses included in this study. Although the stimuli presented to selected sites disrupted for 100–200 ms, the regular theta rhythm identified in the recorded local field potentials, the rhythm reappeared in phase afterward (Gruart et al. 2006).

Animals included in the context group did not present any CR (Fig. 2D). Pseudoconditioned animals presented a low number (<10%) of CRs during the pseudoconditioning sessions—i.e., at a rate similar to values presented during habituation and extinction sessions. Obviously, the pseudoconditioned group failed to reach criterion (>70% of CRs) by the 10th conditioning session (Fig. 2C,E). For the animals included in the

trace group, the percentage of CRs increased rapidly across conditioning, reaching 50% by the third conditioning session and asymptotic values (90%) from the 7th to the 10th conditioning sessions. The trace group presented CR values significantly larger than those collected during habituation from the 3rd to the 10th conditioning sessions [$F_{10,54} = 51.352$; $P < 0.001$; Fig. 2C,F]. Finally, the delay group acquired their conditioning paradigm even faster than the trace group, reaching percentages of CRs significantly different from habituation values from the 2nd to the 10th conditioning sessions [$F_{10,54} = 24.677$; $P < 0.001$; Fig. 2C,G].

Analysis of the Evolution of Evoked Fepsp Across Training Sessions

In order to facilitate the interpretation of the collected results, we will explain here a representative example of the changes taking place at the 6 selected hippocampal synapses across the successive training sessions in the 4 experimental groups. Specifically, in Figure 3 are illustrated the changes in synaptic strength taking place at the DG-CA3 synapse in the trace conditioning group.

In accordance with an early study (Weisz et al. 1984), fEPSPs evoked by the electrical stimulation of the perforant pathway changed in slope in the trace conditioning group (taking the slope of fEPSPs collected during the 2 habituation sessions as 100%) across conditioning sessions. However, those changes could represent either an increase or a decrease with respect to baseline values. As illustrated in Figure 3A, fEPSPs recorded at different sites corresponding to the DG-CA3 synapse either increase (left set of recordings) or decrease (right set of recordings) across the training. A quantitative analysis of the first recording site (Fig. 3A, $+\Delta$ electrode, and Fig. 3C, black triangles) showed fEPSPs significantly larger [$F_{7,127} = 71.514$; $P < 0.001$] than baseline (habituation) values from the 6th to the 10th conditioning sessions and for the 5 extinction sessions. Similarly, the second recording site (Fig. 3A, $-\Delta$ electrode, and Fig. 3C, white triangles) evoked fEPSPs significantly smaller [$F_{6,111} = 47.628$; $P < 0.001$] than baseline values from the 5th to the 10th conditioning sessions and for the 5 extinction sessions. In Figure 3D is represented the evolution at 5 recording sites corresponding to the DG-CA3 synapse, presenting fEPSPs that increased ($+\Delta$) significantly ($P \leq 0.01$) in slope across conditioning, and another 5 recording sites presenting fEPSPs that decreased ($-\Delta$) significantly ($P \leq 0.01$) in slope across training. Following 2 previous studies (Whitlock et al. 2006; Fernández-Lamo et al. 2009), we also considered those recording sites that did not change significantly in slope across training (i.e., when regression analysis applied to the collected slopes did change <±1 SD). Using this analytical procedure, we found that for the DG-CA3 synapse, 40% (6 of 15) of the recording electrodes showed a significant increase ($P \leq 0.01$) in slope across conditioning sessions, while 33.3% (5 of 15) presented decreasing ($P \leq 0.01$) fEPSP slopes, and 26.7% (4 of 15) presented no significant changes. The polynomial regressions shown in Figure 3E correspond to the algebraic mean [$([+\Delta] + [-\Delta])/N$] of data collected from electrodes (N) presenting significant changes during conditioning sessions. The regression illustrated in Figure 3E is a good representation of changes in synaptic strength taking place in the DG-CA3 synapse during trace conditioning in behaving rabbits.

Changes in Synaptic Strength Taking Place in the 6 Selected Synapses During the 4 Experimental Procedures

All of the recorded changes in fEPSP slopes for the 6 hippocampal synapses included in this study and collected during the 4 training protocols (context, pseudoconditioning, and trace and delay conditioning paradigms) were analyzed as already illustrated in Figure 3 for the DG-CA3 synapse during a trace conditioning paradigm. As shown in Figure 4, the increase in the percentage of CRs (Fig. 4A) and the change [$([+\Delta] + [-\Delta])/N$] in synaptic strength taking place at each selected synapse (Fig. 4B) were transduced into a color code. Thus, in Figure 4C–F, we show the increase in the percentage of CRs (isolated left bar in C-F) and the changes in fEPSP slopes taking place in the 6 selected synapses (PP-DG, PP-CA3, PP-CA1, DG-CA3, CA3-CA1, and CA3-cCA1) during context (C), pseudoconditioning (D), and trace (E) and delay (F) conditioning paradigms. For the sake of clarity, the same fEPSP results collected from the 6 synapses are represented in Figure 5 in the form of best polynomial fit ($r \geq 0.81$; $P \leq 0.01$) for context (A1), pseudoconditioning (B1), and trace (C1) and delay (D1) conditioning. A minimum of 15 recording electrodes/selected synapse presenting absolute changes in strength were included in the analysis illustrated in Figures 4 and 5.

Just placing experimental animals in the restraining box for up to 17 sessions (context group) evoked significant ($P \leq 0.007$) changes in fEPSP slopes (Fig. 4C) at selected synapses and at different times across training. The most noticeable increase in activity took place at the PP-DG synapse in the very first sessions of the training. Similar increases in fEPSP slopes were also observed in the CA3-CA1 and CA3-cCA1 synapse, but for a short period of time. The most-significant ($P \leq 0.01$) and longest lasting changes in synaptic strength took place at the 3 input synapses (PP-DG, PP-CA3, PP-CA1) representing an input to the hippocampal intrinsic circuit. It should be pointed out that the increased activity observed in hippocampal synapses during the first training sessions decreased with time (Figs 4C and 5A1).

The pseudoconditioning group also presented sustained ($P \leq 0.01$) changes in the 3 input synapses (PP-DG, PP-CA3, PP-CA1) to the hippocampal intrinsic circuit during the first 10–12 training sessions (Fig. 4D). Similar increases in synaptic strength, but of a shorter duration, were also observed in the CA3-CA1 and CA3-cCA1 synapses (Fig. 4D). As already indicated for the context group, the slopes of fEPSPs evoked at the 6 selected synapses during pseudoconditioning decreased progressively with training, reaching the lowest values during the last 2 training sessions (Figs 4D and 5B1).

During trace conditioning, animals presented very interesting changes in absolute synaptic strength (Fig. 4E). First, major changes took place across the training (i.e., during both conditioning and extinction) sessions. Major significant ($P \leq 0.01$) changes in synaptic strength were observed not only in the PP-DG synapse, but also in some of the synapses included in the hippocampal intrinsic circuit (DG-CA3, CA3-CA1, and CA3-CA1c). Other synapses (PP-CA3 and PP-CA1) were apparently less involved in the acquisition of this trace conditioning paradigm. Some synapses (PP-DG, DG-CA3, and CA3-CA1) were still very active during the last extinction sessions (Fig. 4E).

Finally, during delay conditioning (Fig. 4F), we observed changes in synaptic strength not exactly equal to those noticed during trace conditioning. For example, in this case, the synapses presenting the highest rate of change ($P \leq 0.01$) were 2
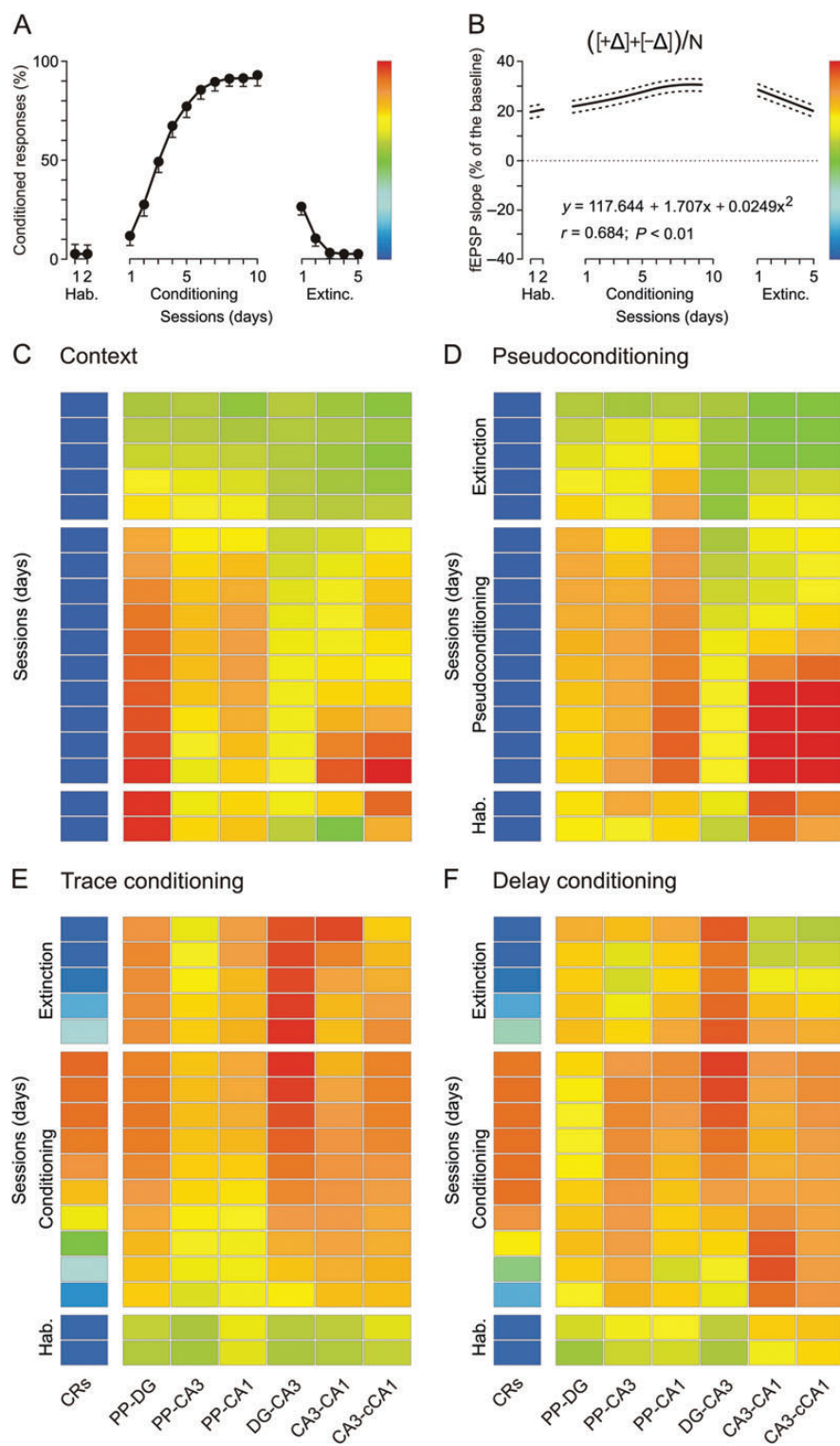
Figure 4. Evolution of fEPSP slopes at 6 different synapses of the hippocampal intrinsic circuit during the 4 selected conditioning situations. (*A,B*) Evolution of CRs (*A*) and of fEPSP slopes evoked at the CA3-cCA1 synapse (*B*) across conditioning sessions using a trace paradigm (*n* = 6 animals). Illustrated fEPSP regression curves were averaged [([+Δ] + [−Δ])/N] from 15 electrodes implanted in the cCA1 area. The equation corresponding to the best polynomial fit to data collected during conditioning sessions is indicated, as well as the corresponding regression curve and the simultaneous 95% confidence bands. Note the color code bars located to the right of (*A*) and (*B*) panels. (*C–F*) Evolution of CRs (%) and of fEPSP slopes (as % of baseline values, see (*B*)) collected at 6 hippocampal synapses across the successive training sessions in 4 different experimental situations: context (no CS or US presentations, (*C*)), pseudoconditioning (*D*), and trace (*E*) and delay (*F*) conditioning paradigms. In the case of context (*C*) and pseudoconditioning (*D*), we took as baseline the values of fEPSP slopes collected during the last 2 (14th and 15th) training sessions. In contrast, baseline values for fEPSP slopes in trace (*E*) and delay (*F*) conditioning were collected from the first two (habituation) sessions.
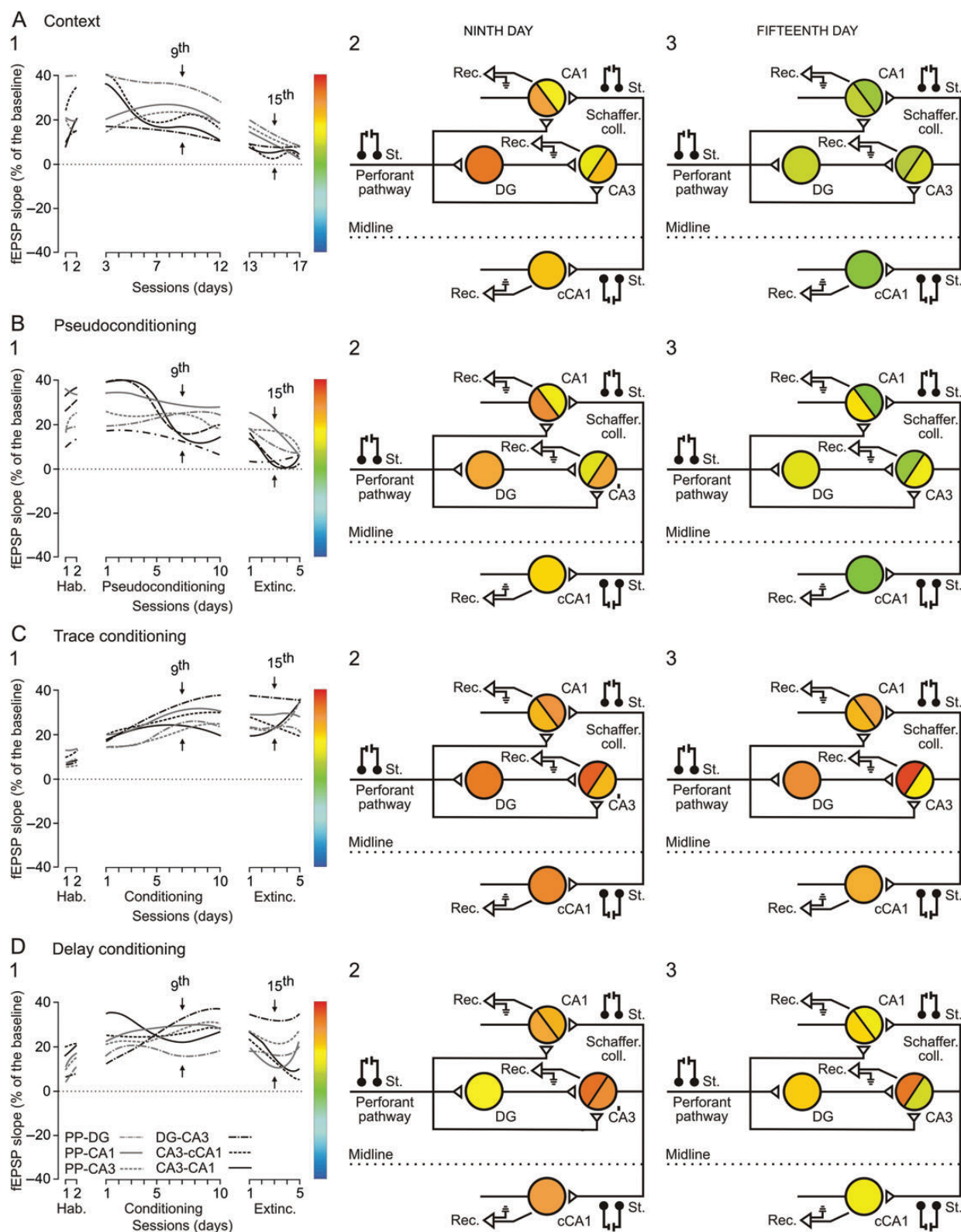
Figure 5. Main changes in synaptic strength evoked in the hippocampal circuit by context and cues present during classical eyeblink conditioning tasks. (A–D) Evolution of fEPSP slopes at the 6 selected synapses during context (A), pseudoconditioning (B), and trace (C) and delay (D) conditioning. For (A–D) in **1** are illustrated the best polynomial fits ($r \geq 0.81$; $P \leq 0.01$) for the fEPSP data collected from the 6 selected synapses (see line codes in **D1**), while in **2–3** are represented the synaptic strength corresponding to each synapse and collected during the 9th (corresponding to the 7th conditioning or pseudoconditioning session; see arrows) and 15th (corresponding to the third extinction session; see arrows) recording days. The corresponding color codes are represented to the right of panels **1** (for A–D). Note that for context, the major changes in the 9th training session were observed at the PP-DG and—with lower intensity—the PP-CA3 and PP-CA1 synapses. Similar results were collected in the 9th training session from pseudoconditioned rabbits. In contrast, during the equivalent training session for trace conditioning, major changes in synaptic strength were observed not only in the input synapses to the hippocampus (PP-DG, PP-CA3, and PP-CA1), but also in the intrinsic circuit (DG-CA3, and to a lower degree in CA3-CA1 and CA3-cCA1 synapses). Similar results were collected during delay conditioning.

located in the hippocampal intrinsic circuit—DG-CA3 and CA3-CA1—although the changes in the former took place later than those in the latter. Interestingly enough, some seminal studies (Segal and Olds 1972; Segal et al. 1972) did report changes in the CA3-CA1 synapse not dependent upon those taking place in the DG, using a tone-food association test. Finally, smaller changes in strength were also observed in synapses corresponding to hippocampal inputs (PP-CA3) and the hippocampal commissural pathway (CA3-cCA1).

Functional State of Hippocampal Circuits at a Given Moment Across Training

Figure 6 represents an attempt to display the functional state of the hippocampal circuits included in this study at a similar moment (i.e., the 9th and the 15th recording days) across training in the 4 experimental situations considered here: context (Fig. 5A2,3), pseudoconditioning (Fig. 5B2,3), and trace (Fig. 5C2,3), and delay (Fig. 5D2,3) conditionings. Results included in these diagrams illustrate clearly the different functional states in which hippocampal circuits are placed during these 4 experimental situations. For example, in both context and pseudoconditioning, peak changes by the 9th recording day were observed at synapses afferent to hippocampal circuits (mainly PP-DG, and to a lesser degree PP-CA3 and PP-CA1). In contrast, by the same recording day (corresponding to the 7th

Figure 6. A diagrammatic representation of the major changes in synaptic strength taking place in hippocampal inputs and intrinsic circuit during context and pseudoconditioning (A) and during trace and delay conditioning (B).

conditioning session in conditioned animals), the main changes in synaptic strength taking place during both trace and delay conditioning also involved synapses located in the hippocampal intrinsic circuit (i.e., DG-CA3, CA3-CA1) or in the commissural pathway (CA3-cCA1). Differences were even more noticeable during the 15th training day (corresponding to the third extinction session in conditioned animals), because most hippocampal synapses presented the lowest changes in strength in both context and pseudoconditioning groups, while considerable changes in strength were still taking place in the hippocampal circuit in both trace (mostly PP-DG, DG-CA3, and CA3-CA1 synapses) and delay (mostly in the DG-CA3 synapse) during this (third) extinction session. Similar results are obtained considering the functional status of each selected synapse for a given day and training situation (see Fig. 4C–F). Thus, the hippocampus seems to present a different functional state for each experimental situation and even for each day, across the successive training sessions.

Discussion

General Remarks

We have shown here that hippocampal synapses included in the main afferent inputs and intrinsic circuit are involved in selective processes related not only to the acquisition and extinction of different forms (trace and delay) of classical eyeblink conditioning, but also in more general aspects of the learning situation—namely those related to environmental settings and to the unpaired presentations of CS and US. The 6 different hippocampal synapses included in this study underwent a slow algebraic modulation (i.e., increase or decrease) in synaptic strength (Konorski 1948; Hebb 1949) across the different training situations in parallel (as shown by nonlinear regression analyses) with the acquisition and extinction of conditioned eyelid responses and/or the mere repetition of sessions (context and pseudoconditioning). Interestingly, changes in synaptic weights did not take place simultaneously in the 6 selected synaptic sites nor presented similar absolute changes in strength across the successive training sessions. Obviously, this new picture of differential plastic changes taking place in different hippocampal synapses in a given experimental situation and in a precise moment across the training situation was not possible to observe if only one synapse was observed (Weisz et al. 1984; Gruart et al. 2006; Whitlock et al. 2006). In addition, present results convincingly suggest that a specific functional synaptic state corresponds to each learning paradigm and training session (Fig. 5). In particular, direct projections from the entorhinal cortex to the 3 main neuronal elements of the hippocampal intrinsic circuit (i.e., PP-DG, PP-CA3, and, to a lesser degree, PP-CA1 synapses) seemed to be mostly involved in general and/or contextual aspects of the training situation, while those synapses integrating the intrinsic circuit (DG-CA3, CA3-CA1, and CA3-cCA1) were preferentially involved in aspects related to CS predictive value and/or CS-US associative strength (see Fig. 6; Rescorla 1988; Eichenbaum 1999; Múnera et al. 2001).

Separate Roles of Hippocampal Inputs and Intrinsic Circuit

The separation of functions between entorhinal projections to the hippocampus and hippocampal synapses involved in its
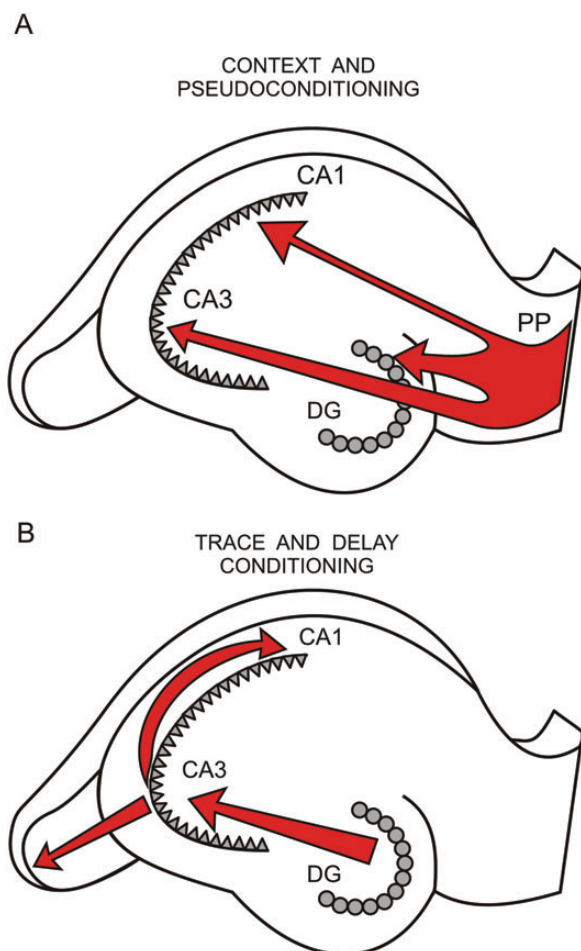
intrinsic circuit reported here has already been proposed on both theoretical (Marr 1971; McNaughton and Morris 1987; Treves and Rolls 1994) and experimental (McHugh et al. 2007; McHugh and Tonegawa 2009; Nakashiba et al. 2012) grounds. In short, direct projections from the entorhinal cortex to the dentate granule neurons and to hippocampal CA3 and CA1 pyramidal cells will carry memory information related to general environmental aspects, places, and other spatial-temporal details and configurations. The proportionally large number of dentate granule neurons will allow the proper separation of these sensory-motor and cognitive memories. As shown here, those incoming entorhinal patterns of activity not involved in Hebbian association processes (Konorski 1948; Hebb 1949) will be erased and/or blocked at these 3 (PP-DG, PP-CA3, and PP-CA1) hippocampal synapses. Similar filtering and/or erasing roles have already been proposed for the dentate gyrus (Hsu 2007; McHugh et al. 2007; Nakashiba et al. 2012), and the hippocampal CA3 (McHugh and Tonegawa 2009) and CA1 (Izumi and Zorumski 2008) areas. In contrast, synapses involved in the hippocampal intrinsic circuit (represented here by the DG-CA3, CA3-CA1, and CA3-cCA1 synapses) will play a discriminant role, reinforcing Hebbian association between relevant environmental stimuli (Vinogradova 2001; Hsu 2007), such as, for example, that taking place between CS and US presented in a paired form during both trace and delay paradigms. It has been proposed that this selective role of the hippocampal intrinsic synapses will be supported on the dense network of axon collaterals reaching both CA3 and CA1 pyramidal neurons (Lorente de Nó 1933, 1934; Marr 1971; Amaral 1993). Currently, it is assumed that these recurrent connections will probably help to determine the CS cognitive salience and/or the CS-US associative strength. This conceptual approach to hippocampal functions is further support by data provide here (see Figs 4 and 5). In addition, Figure 6 attempts to represent in a diagrammatic form these important functional differences and specific roles of hippocampal inputs and that of its intrinsic circuit.

Involvement of the Hippocampus in the Acquisition of Classical Conditioning of Eyelid Responses

In an early, seminal study, Weisz et al. (1984) demonstrated a change in the strength of synaptic activation of dentate granule cells by perforant pathway axons during the acquisition of nictitating membrane CRs in behaving rabbits. This activity-dependent modulation in synaptic strength was further confirmed for the CA3-CA1 synapse of behaving mice, and extended to the extinction process (Gruart et al. 2006), suggesting that the 2 phenomena are equally active (Dudai 2012). Moreover, it has also been shown that the changes in synaptic efficacy evoked in the hippocampal CA3-CA1 synapse present a linear relationship with the amount of acquired, or extinguished, learning (Gruart et al. 2006). The increase in fEPSP slope during the acquisition process explains the increased firing in hippocampal CA1 areas across conditioning, described for both rabbits (McEchron et al. 2003) and cats (Múnera et al. 2001).

The involvement of hippocampal unitary activity in classical conditioning of the nictitating membrane/eyelid responses was reported years ago (Berger et al. 1983; Moyer et al. 1990). Hippocampal pyramidal cell firing to CS presentation increases several sessions in advance of behavioral conditioning (McEchron and Disterhoft 1997). Although it has been shown that

the discharge rate of hippocampal CA1 pyramidal neurons does not encode the kinematic peculiarities of conditioned eyelid responses (Múnera et al. 2001; Sánchez-Campusano et al. 2007), discharge rates of CA1 pyramidal cell firing appear linearly related to the progressive acquisition of CRs, with a gain of ≈ 0.035 spikes/s/trial, as measured in behaving cats during trace conditioning (Múnera et al. 2001). It is of note that this slow building up of hippocampal neuronal firing responses across conditioning sessions is similar to the maximum increases in fEPSP slopes evoked at the 6 synapses included in this study (i.e., ≈0.03–0.04% increase in fEPSP slope/trial). A similar increase in the slope of fEPSPs recorded in the CA3-CA1 synapse during trace (tone-shock) conditioning of behaving mice has also been reported (Gruart et al. 2006). Taken together, these results suggest that changes in neuronal firing rates across conditioning sessions are more-or-less related to the underlying changes in synaptic efficacy.

Although it has been pointed out (Moyer et al. 1990) that 250-ms trace conditioning is not dependent of the hippocampus in the rabbit, results collected here (Figs 4 and 5) convincingly shown that hippocampal circuits are also modified by this type of associative learning task.

The decrease in synaptic strength taking place in different recording sites in both input and intrinsic hippocampal synapses could be related to the recently reported increase in intrinsic excitability on hippocampal interneurons (McKay et al. 2013).

Functional Synaptic States Underlying Hippocampal Roles in Associative Learning

It has already been proposed (Delgado-García and Gruart 2002) that learning is a precise functional state of the brain, and that we should take a dynamic approach to the study of neural and synaptic activities in ensembles of sensorimotor circuits during actual learning in alert behaving animals. The color diagrams included in Figure 5A–D are a good illustration of the above contention, showing the significantly different synaptic weights presented by the 6 selected hippocampal synapses on the same training days, but in 4 different conditioning situations (i.e., context, pseudoconditioning, and trace and delay conditioning paradigms). In general, it can be proposed that each environmental and social situation demanding a behavioral response will evoke a corresponding differential state of synaptic weights in hippocampal circuits. Obviously, additional neural, synaptic, and motoric information can be collected experimentally and added to the better determination of ongoing functional states. For example, and with regard to classical eyeblink conditioning, it has already been reported that facial motoneurons present 2 specific functional states corresponding to their firing activities during reflexively evoked blinks and to their discharge rate during acquired (i.e., classically conditioned) eyelid responses (Delgado-García and Gruart 2006). However, it is important to point out that our information with regard to brain functioning during a given learning situation is greatly constrained by the difficulty of recording a large enough number of kinetic (i.e., firing and synaptic activities of neuronal elements) and kinematic (i.e., biomechanical characteristics of evoked motor responses) parameters in simultaneity with the newly acquired ability (Delgado-García and Gruart 2002). To solve these constraints, it seems necessary to record enough different neural kinetic data at the same time as

collecting data from enough kinematic variables. In a previous study, we were able to collect up to 24 kinetic variables (related to neural firing activities in the facial and cerebellar interpositus nuclei) together with 36 kinematic variables (related to eyelid biomechanics and to the electrical activity of the orbicularis oculi muscle) from alert behaving cats during classical eyeblink conditioning (Sánchez-Campusano et al. 2007). Present results further confirm the above contentions, and allow a dynamic interpretation of the hippocampal role in learning and memory processes underlying the acquisition of new motor and cognitive abilities, as opposed to an excessive localizationist view of hippocampal functions (McHugh et al. 2007). The hippocampus will have an almost infinite repertoire of functional states corresponding to the enormous possibilities of sensory stimulations and the different needs of behavioral responses. Thus, and depending on the specific and timed activation of its multiple synaptic contacts, the hippocampus would be involved in many different functions, such as object recognition (Clarke et al. 2010), spatial orientation (Moser et al. 2008), and other different forms of memory acquisition, storage, and retrieval (Bliss and Collingridge 1993; Neves et al. 2008; Wang and Morris 2010).

Funding

Notes

References

Amaral DG. 1993. Emerging principles of intrinsic hippocampal organization. Curr Opin Neurobiol. 3:225–229.

Andersen P, Blackstad TW, Lømo T. 1966a. Location and identification of excitatory synapses on hippocampal pyramidal cells. Exp Brain Res. 1:236–248.

Andersen P, Holmqvist B, Voorhoeve PE. 1966b. Entorhinal activation of dentate granule cells. Acta Physiol Scand. 66:448–460.

Berger TW, Rinaldi P, Weisz DJ, Thompson RF. 1983. Single-unit analysis of different hippocampal cell types during classical conditioning of rabbit nictitating membrane response. J Neurophysiol. 50:1197–1219.

Bliss TVP, Collingridge GL. 1993. A synaptic model of memory: long-term potentiation in the hippocampus. Nature. 361:31–39.

Bliss TVP, Lømo T. 1973. Long-lasting potentiation of synaptic transmission in the dentate area of the anesthetized rabbit following stimulation of the perforant path. J Physiol (Lond). 232:331–356.

Clarke JR, Cammarota M, Gruart A, Izquierdo I, Delgado-García JM. 2010. Plastic modifications induced by object recognition memory processing. Proc Natl Acad Sci USA. 107:2652–2657.

Delgado-García JM, Gruart A. 2006. Building new motor responses: eyelid conditioning revisited. Trends Neurosci. 29:330–338.

Delgado-García JM, Gruart A. 2002. The role of interpositus nucleus in eyelid conditioned responses. Cerebellum. 1:289–308.

Dudai Y. 2012. The restless engram: consolidations never end. Annu Rev Neurosci. 35:227–247.

Eichenbaum H. 1999. Conscious awareness, memory and the hippocampus. Nat Neurosci. 2:775–776.

Fernández-Lamo I, Montero-Pedrazuela A, Delgado-García JM, Guadaño-Ferraz A, Gruart A. 2009. Effects of thyroid hormone replacement on associative learning and hippocampal synaptic plasticity in adult hypothyroid rats. Eur J Neurosci. 30:679–692.

Girgis M, Shih-Chang W. 1981. A new stereotaxic atlas of the rabbit brain. St. Louis, MO: Warren H. Green.

Gruart A, Muñoz MD, Delgado-García JM. 2006. Involvement of the CA3-CA1 synapse in the acquisition of associative learning in behaving mice. J Neurosci. 26:1077–1087.

Gruart A, Schreurs BG, Domínguez del Toro ED, Delgado-García JM. 2000. Kinetic and frequency-domain properties of reflex and conditioned eyelid responses in the rabbit. J Neurophysiol. 83:836–852.

Hebb DO. 1949. The organization of behavior. New York (NY): Wiley.

Hsu D. 2007. The dentate gyrus as a filter or gate: a look back and a look ahead. Prog Brain Res. 163:601–613.

Izumi Y, Zorumski CF. 2008. Direct cortical inputs erase long-term potentiation at Schaffer collateral synapses. J Neurosci. 28:9557–9563.

Kandel ER. 2001. The molecular biology of memory storage: a dialogue between genes and synapses. Science. 294:1030–1038.

Konorski J. 1948. Conditioned reflexes and neuron organization. Cambridge (MA): Cambridge University Press.

Leal-Campanario R, Fairén A, Delgado-García JM, Gruart A. 2007. Electrical stimulation of the rostral medial prefrontal cortex in rabbits inhibits the expression of conditioned eyelid responses but not their acquisition. Proc Natl Acad Sci USA. 104:11459–11464.

Lømo T. 1971a. Patterns of activation in the monosynaptic cortical pathway: the perforant path input to the dentate area of the hippocampal formation. Exp Brain Res. 12:18–45.

Lømo T. 1971b. Potentiation of monosynaptic EPSPs in the perforant path-dentate granule cell synapse. Exp Brain Res. 12:46–63.

Lorente de Nó R. 1933. Studies on the structure of the cerebral cortex. I. The area entorhinalis. J Psychol Neurol (Lpz). 45:381–438.

Lorente de Nó R. 1934. Studies on the structure of the cerebral cortex. II. Continuation of the study of the ammonic system. J Psychol Neurol (Lpz). 46:113–177.

Marr D. 1971. Simple memory: a theory for archicortex. Philos Trans R Soc Lond B Biol Sci. 262:23–81.

McEchron MD, Disterhoft JF. 1997. Sequence of single neuron changes in CA1 hippocampus of rabbits during acquisition of trace eyeblink conditioned responses. J Neurophysiol. 78:1030–1044.

McEchron MD, Tseng W, Disterhoft JF. 2003. Single neurons in CA1 hippocampus encode trace interval duration during trace heart rate (fear) conditioning in rabbit. J Neurosci. 23:1535–1547.

McHugh TJ, Jones MW, Quinn JJ, Balthasar N, Coppari R, Elmquist JK, Lowell BB, Fanselow MS, Wilson MA, Tonegawa S. 2007. Dentate gyrus NMDA receptors mediate rapid pattern separation in the hippocampal network. Science. 317:94–99.

McHugh TJ, Tonegawa S. 2009. CA3 NMDA Receptors are required for the rapid formation of a salient contextual representation. Hippocampus. 19:1153–1158.

McKay BM, Oh MM, Disterhoft JF. 2013. Learning increases intrinsic excitability of hippocampal interneurons. J Neurosci. 33:5499–5506.

McNaughton BL, Morris RGM. 1987. Hippocampal synaptic enhancement and information storage within a distributed memory system. Trends Neurosci. 10:408–415.

Moser EI, Kropff E, Moser MB. 2008. Place cells, grid cells, and the brain's spatial representation system. Rev Neurosci. 31:69–89.

Moyer JR Jr, Deyo RA, Disterhoft JF. 1990. Hippocampectomy disrupts trace eye-blink conditioning in rabbits. Behav Neurosci. 104:243–252.

Múnera A, Gruart A, Muñoz MD, Fernández-Más R, Delgado-García JM. 2001. Discharge properties of identified CA1 and CA3 hippocampus neurons during unconditioned and conditioned eyelid responses in cats. J Neurophysiol. 86:2571–2582.

Nakashiba T, Cushman JD, Pelkey KA, Renaudineau S, Buhl DL, McHugh TJ, Rodriguez-Barrera V, Chittajallu R, Iwamoto KS, McBain CJ et al. 2012. Young dentate granule cells mediate pattern separation, whereas old granule cells facilitate pattern completion. Cell. 149:188–201.

Neves G, Cooke SF, Bliss TV. 2008. Synaptic plasticity, memory and the hippocampus: a neural network approach to causality. Nat Rev Neurosci. 9:65–75.

Porras-García E, Sánchez-Campusano R, Martínez-Vargas D, Domínguez-del-Toro E, Cendelín J, Vožeh F, Delgado-García JM. 2010. Behavioral characteristics, associative learning capabilities, and dynamic association mapping in an animal model of cerebellar degeneration. J Neurophysiol. 104:346–365.

Ramón y Cajal S. 1909–1911. Histologie du système nerveux de l'homme et des vertébrés. Paris, France: Malonie.

Rescorla RA. 1988. Behavioral studies of Pavlovian conditioning. Annu Rev Neurosci. 11:329–352.

Sánchez-Campusano R, Gruart A, Delgado-García JM. 2007. The cerebellar interpositus nucleus and the dynamic control of learned motor responses. J Neurosci. 27:6620–6632.

Segal M, Disterhoft JF, Olds J. 1972. Hippocampal unit activity during classical aversive and appetitive conditioning. Science. 175:792–794.

Segal M, Olds J. 1972. Behavior of units in hippocampal circuit of the rat during learning. J Neurophysiol. 35:680–690.

Treves A, Rolls ET. 1994. Computational analysis of the role of the hippocampus in memory. Hippocampus. 4:374–391.

Vinogradova OS. 2001. Hippocampus as comparator: role of the two input and two output systems of the hippocampus in selection and registration of information. Hippocampus. 11:578–598.

Wang SH, Morris RG. 2010. Hippocampal-neocortical interactions in memory formation, consolidation, and reconsolidation. Annu Rev Psychol. 61:49–79.

Weisz DJ, Clark GA, Thompson RF. 1984. Increased responsivity of dentate granule cells during nictitating membrane response conditioning in rabbit. Behav Brain Res. 12:145–154.

Whitlock JR, Heynen AJ, Shuler MG, Bear MF. 2006. Learning induces long-term potentiation in the hippocampus. Science. 313:1093–1097.